Noname manuscript No.
(will be inserted by the editor)

Attitude Determination of Multirotor Aerial Vehicles Using Camera Vector Measurements

Davi A. Santos · Pedro F. S. M. Gonçalves

Received: date / Accepted: date

Abstract The employment of embedded cameras in navigation and guidance of Unmanned Aerial Vehicles (UAV) has attracted the focus of many academic researches. In particular, for the multirotor UAV, the camera is widely employed for applications performed in indoor environments, where the GNSS signal is often unreliable and electromagnetic interference can be a concern. In the literature, images are mostly adopted for position and velocity estimation, rather than attitude estimation. This paper proposes an attitude determination method for multirotor aerial vehicles using pairs of vector measurements taken from a downward-facing strapdown camera. The method is composed of three modules. The first one detects and identifies the visible landmarks by processing the images. The second module computes the vector measurements related to the direction from the camera to the landmarks. The third module estimates attitude from the vector measurements. In the last module, a version of the Multiplicative Extended Kalman Filter (MEKF) with sequential update is proposed as estimation method. The overall method is evaluated via Monte Carlo simulations, showing that it is effective in determining the vehicle's attitude and revealing its properties.

Keywords Multirotor Aerial Vehicle · Multiplicative Extended Kalman Filter · Attitude Determination · Computer Vision

1 Introduction

Recently, unmanned aerial vehicles (UAV) have becoming more and more common in our daily lives. Nowadays, these devices find applications in situations which would involve risk or be too expensive for a human pilot. Some of the applications found in the literature are agricultural management [13], topography

D. A. Santos · P. F. S. M. Gonçalves
Instituto Tecnológico de Aeronáutica, Praça Marechal Eduardo Gomes, 50, Vila das Acácias, 12228-900, São José dos Campos, São Paulo, Brazil
Tel.: +55-12-39476980
Corrersponding author: D. A. Santos
E-mail: davists@ita.br

reconstruction [16], surveillance and exploration of disaster areas [24], and soil erosion monitoring [17]. In particular, the multirotor-type UAVs are highly suitable for the aforementioned applications thanks to their hovering and low-speed flight capability, vertical take-off and landing (VTOL), and high maneuverability [26].

The multirotor UAV needs feedback controllers in order to achieve stability. Typically, the multirotor controller is organized in two loops: the internal loop, concerned with the attitude control; and the external loop, which is governed by the position controller, which in turn commands the internal loop [19]. In order to provide feedback for the attitude controller, a control system for multirotor vehicles requires attitude determination (AD), whose function is to estimate the vehicle's attitude (orientation) by processing the measurement signals of appropriate sensors (rate-gyros, accelerometers, magnetometers, etc.).

The research on AD in the aerospace community has a long history. In fact, it acquired a formal aspect in [25], where the classical problem of attitude determination from vector measurements was first defined. The reference [27] describes the first AD methods, classifying them into two categories: batch methods and recursive methods. Besides this classification, the AD methods can be classified according to the attitude parameterization they adopt. Euler angles and quaternions of rotation are the preferred attitude parameterizations. Euler angles allows an ease 3D visualization. On the other hand, quaternions have the lowest dimensionality (four) among the nonsingular parameterizations. A survey of attitude parameterizations is found in [21].

The first batch methods proposed for AD were the QUEST and the TRIAD [22]. In these methods, the attitude is estimated using measurements of the present time instant, discarding past measurements. In order to determine three-axis attitude, these methods require measurements from at least two physical vectors, *e.g.* the gravity and the geomagnetic field density. If only one vector is considered, the attitude stay undetermined around its direction.

In its turn, the recursive methods for AD can be divided into two groups, depending on their underlying estimation criterion: Least Squares (LS) methods; and Minimum Variance (MV) methods. Examples of quaternion estimators using the LS criterion can be found in [1] and [6]. The Additive Extended Kalman Filter (AEKF) [2] and the Multiplicative Extended Kalman Filter (MEKF) [15] are examples of MV methods, also using the quaternions as attitude representation. The filter presented in [8] is an example of MV method using Euler angles as attitude representation.

The inertial sensors usually adopted in multirotor vehicles are low-cost microelectromechanical systems (MEMS). These devices provide quite noisy measurements and, for this reason, they often require auxiliary sensors. Particularly, one can note that, together with the gravity vector, the accelerometers measure the vehicle's lateral acceleration and its vibration, which insert errors in the vector measurements. To compensate those errors, the reference [9] estimates the vehicle's lateral acceleration using a GPS receiver, while the reference [14] uses a second order infinite impulse response (IIR) notch filter for rejecting the effects of vibration. Although, in practice, the Kalman filter is quite commonly used for multirotor attitude estimation, there are still few works in the literature reporting them in detail; one can cite the following two papers: [26] and [12]. It is also worth pointing out that the results concerning the problem of AD from vector mea-

surements, as they were proposed in the aerospace literature, are to some extent ignored in the recent literature on aerial robotics.

In the sequel, we review some works which deals with camera for state estimation in UAVs. The references [5] and [7] present filters that fuses accelerometer and rate-gyro data with images from a single camera to estimate the position, the attitude, and the velocity of a conventional helicopter UAV. In both works, the camera is fixed on the vehicle structure and faces one target with known position on the floor. The reference [4] fuses stereo visual odometry with inertial measuremets using a Kalman filter for estimating the position and velocity of a quadrotor UAV. The reference [20] presents a clear and extensive review about motion estimation based on camera measurements, using different approaches, starting from horizon-based methods and passing through vanishing points, optical flow, and stereoscopic methods. For indoor and urban applications, the reference [23] adopts a catadioptric optical system for attitude estimation.

The present work recall the classical problem of attitude determination from vector measurements [25] to propose an attitude determination method appropriate for aerial robots, like multirotor vehicles. In our method, a single camera together with a set of known landmarks are used to generate a set of noncollinear vector measurements, each one corresponding to the direction from the camera center to one of the landmarks. The state estimator adopted in this method is a modified version of the MEKF [15]. The modification consists of a sequential scheme, at each sample time, for updating the attitude estimates using just one vector measurement per iteration. The remaining text is organized as follows. Section 2 defines the main problem of the paper. Section 3 describes the attitude determination method proposed to solving the paper's main problem. Section 4 evaluates the proposed attitude determination method on the basis of Monte Carlo simulations. Finally, Section 5 presents the paper's conclusions.

2 The Attitude Determination Problem

Consider the multirotor helicopter and the two Cartesian Coordinate Systems (CCS) illustrated in Fig. 1. The body CCS $S_{\mathrm{B}} \triangleq \{X_{\mathrm{B}}, Y_{\mathrm{B}}, Z_{\mathrm{B}}\}$ is attached to the vehicle structure, at its center of mass (CM) and has its z-axis, Z_{B}, perpendicular to the rotor plane. The reference CCS $S_{\mathrm{R}} \triangleq \{X_{\mathrm{R}}, Y_{\mathrm{R}}, Z_{\mathrm{R}}\}$ is fixed on the ground at point O and has its z-axis, Z_{R}, aligned with the local vertical. Fig. 1 also illustrates a set of l landmarks.

Assume that the camera is positioned at CM and there is a triad of rate-gyros installed parallel to S_{B}. Define the set of landmark indices $\mathcal{I} \triangleq \{1, 2, ..., l\}$. Let $i \in \mathcal{I}$ be an arbitrary index. Denote the center of the ith landmark by $M^{(i)}$. Define $\mathbf{s}^{(i)}$ to be the unit geometric vector pointing from CM to $M^{(i)}$. Denote the projections (or representations) of $\mathbf{s}^{(i)}$ in S_{B} and S_{R}, respectively, by $\mathbf{b}^{(i)} \in \mathbb{R}^3$ and $\mathbf{r}^{(i)} \in \mathbb{R}^3$. The representations $\mathbf{b}^{(i)}$ and $\mathbf{r}^{(i)}$ are related by $\mathbf{b}^{(i)} = \mathbf{D}\mathbf{r}^{(i)}$, where $\mathbf{D}$ is the orthonormal attitude matrix of S_{B} with respect to S_{R}.

Assume that the positions of CM and of the landmarks with respect to S_{R} are all known. Assume also that, at instant k, the camera's field of view is such that n landmarks are visible. Denote the indices of such visible landmarks by $i_1, i_2, ..., i_n \in \mathcal{I}$. Based on these assumptions, one can consider the following sequence of pairs of vector measurements:

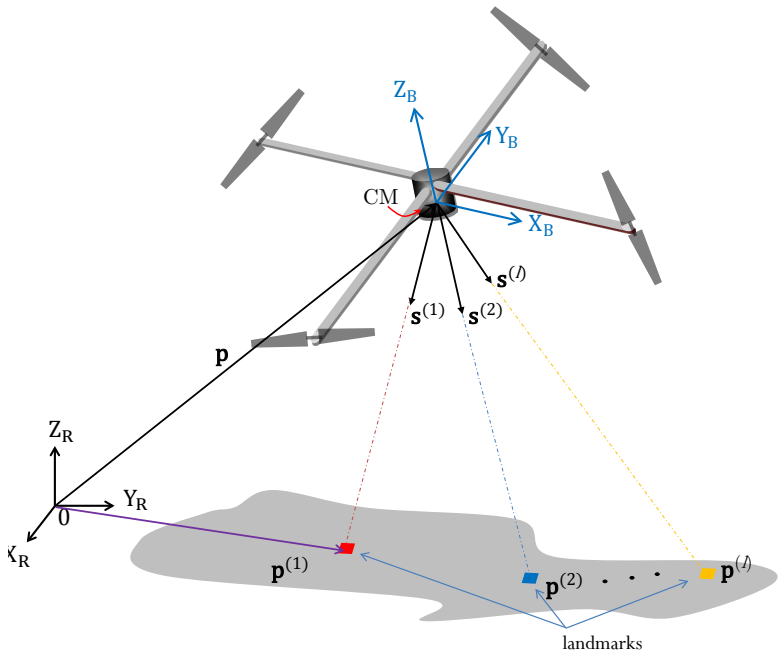

Fig. 1 The Cartesian coordinate systems, the multirotor vehicle, and the flight environment.

$$\mathcal{V}_k \triangleq \left\{ \left(\check{\mathbf{b}}_k^{(i_1)}, \check{\mathbf{r}}_k^{(i_1)} \right), \left(\check{\mathbf{b}}_k^{(i_2)}, \check{\mathbf{r}}_k^{(i_2)} \right), ..., \left(\check{\mathbf{b}}_k^{(i_n)}, \check{\mathbf{r}}_k^{(i_n)} \right) \right\}, \tag{1}$$

where $\check{\mathbf{b}}_k^{(i)}$ and $\check{\mathbf{r}}_k^{(i)}$, for $i = i_1, ..., i_n$, are samples at instant k of $\mathbf{b}^{(i)}$ and $\mathbf{r}^{(i)}$, respectively.

Consider an arbitrary pair of vector measurements at instant k, $\left(\check{\mathbf{b}}_k^{(i)}, \check{\mathbf{r}}_k^{(i)} \right) \in \mathcal{V}_k$, for some $i \in \mathcal{I}$. As a measurement model, assume that the measurements $\check{\mathbf{b}}_k^{(i)}$ and $\check{\mathbf{r}}_k^{(i)}$ are related by:

$$\check{\mathbf{b}}_k^{(i)} = \mathbf{D}(\mathbf{m}_k)\mathbf{r}_k^{(i)} + \delta\mathbf{b}_k^{(i)}, \tag{2}$$

$$\check{\mathbf{r}}_k^{(i)} = \mathbf{r}_k^{(i)} + \delta\mathbf{r}_k^{(i)}, \tag{3}$$

where $\{\delta\mathbf{b}_k^{(i)}\}$ and $\{\delta\mathbf{r}_k^{(i)}\}$ are zero-mean Gaussian white sequences with covariances $\mathbf{R}_{b,k}^{(i)}$ and $\mathbf{R}_{r,k}^{(i)}$, respectively; and $\mathbf{m}_k \in \mathbb{R}^3$ is a sample at instant k of the modified Rodrigues parameters (MRP) that parameterize the attitude matrix $\mathbf{D}$. The expression $\mathbf{D}(\mathbf{m}_k)$ denotes the attitude matrix of S_B with respect to S_R corresponding to $\mathbf{m}_k$:

$$\mathbf{D}(\mathbf{m}_k) = \mathbf{I}_3 + \frac{8[\mathbf{m}_k\times]^2 - 4(1 - \|\mathbf{m}_k\|^2)[\mathbf{m}_k\times]}{(1 + \|\mathbf{m}_k\|^2)^2}, \tag{4}$$

where $[\mathbf{m}_k\times]$ denotes the cross product matrix of $\mathbf{m}_k$.

The attitude kinematics model for the MRP is given by [27]

$$\dot{\mathbf{m}}(t) = \frac{1}{4}\left[\left(1 - \mathbf{m}(t)'\mathbf{m}(t)\right)\mathbf{I}_3 + 2\left[\mathbf{m}(t)\times\right] + 2\mathbf{m}(t)\mathbf{m}(t)'\right]\boldsymbol{\omega}(t), \tag{5}$$

where $\mathbf{m}(t)$ is a continuous-time version of $\mathbf{m}_k$; $\mathbf{m}(t)'$ is the transpose of $\mathbf{m}(t)$; and $\boldsymbol{\omega}(t) \in \mathbb{R}^3$ is the angular velocity of S_{B} with respect to S_{R}.

Let the measurement taken from the triad of rate-gyros at instant k be described by

$$\check{\boldsymbol{\omega}}_k = \boldsymbol{\omega}_k + \delta\boldsymbol{\omega}_k, \tag{6}$$

where $\boldsymbol{\omega}_k \in \mathbb{R}^3$ is a sample of $\boldsymbol{\omega}(t)$ at instant k; and $\{\delta\boldsymbol{\omega}_k\} \in \mathbb{R}^3$ is a zero-mean Gaussian white sequence with covariance $\mathbf{Q}$.

The main problem of the present work is to recursively compute an approximation $\hat{\mathbf{m}}_{k|k}$ of the minimum-variance (MV) estimate of $\mathbf{m}_k$ using the dynamics model (5), the measurement model (2)–(3), the sequence of rate-gyro measurements $\check{\boldsymbol{\omega}}_{1:k} \triangleq \{\check{\boldsymbol{\omega}}_1, \check{\boldsymbol{\omega}}_2, ..., \check{\boldsymbol{\omega}}_k\}$, and the sequence of vector measurements $\mathcal{V}_{1:k} \triangleq \{\mathcal{V}_1, \mathcal{V}_2, ..., \mathcal{V}_k\}$.

3 The Attitude Determination Method

This section proposes an attitude determination method to solve the problem defined in Section 2. The method is structured in a framework consisting of three modules, as illustrated in Fig. 2. Module 1 detects the visible landmarks and computes their positions in image coordinates. Module 2 computes the vector measurement pairs. Module 3 estimates the vehicle's attitude using the vector measurements together with angular velocity measurements.

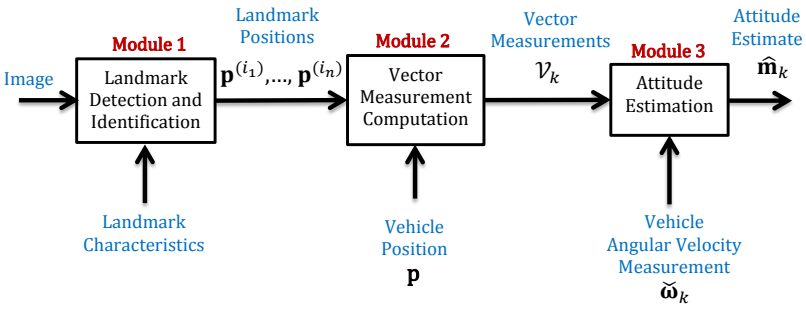

Fig. 2 Block diagram of the overall attitude determination method.

The following three sections detail our choice for each module of the above framework.

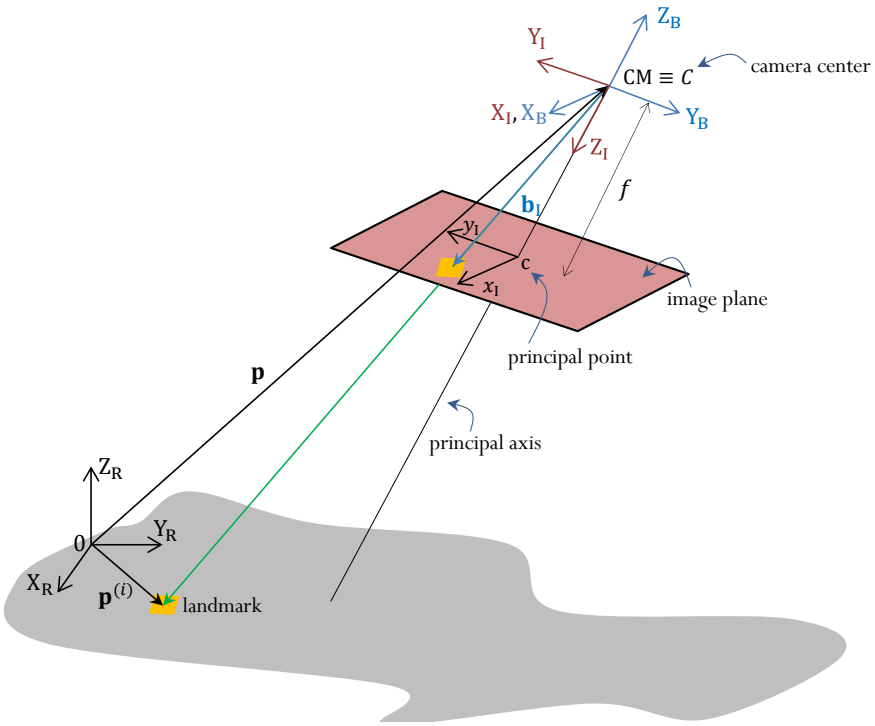

Fig. 3 Vector measurement computation.

3.1 Module 1: Landmark Detection and Identification

As the main contribution of this work is the framework of Fig. 2 itself and the attitude estimation method adopted for module 3, for simplicity, module 1 will be illustrated by means of artificial noise-free color images, avoiding cumbersome issues related to image processing (the reader could refer to [10]). Therefore, a different color is assigned to each landmark and to the image background, allowing detection and identification without errors, by simply reading the image pixels and comparing their RGB color description with the RGB code of the known landmarks.

3.2 Module 2: Vector Measurement Computation

Let $\mathbf{s}$ denote an unit geometric vector pointing from CM to an arbitrary landmark (see the illustration in Fig. 3). Let $(\mathbf{b}, \mathbf{r})$ denote a pair of vector measurements, where $\mathbf{b}$ and $\mathbf{r}$ are vector representations of $\mathbf{s}$ in S_{B} and S_{R}, respectively. Denote the position of CM and the position of the landmark center, both in S_{R}, by $\mathbf{p}$ and $\mathbf{p}^{(i)}$, respectively. Therefore, one can immediately compute

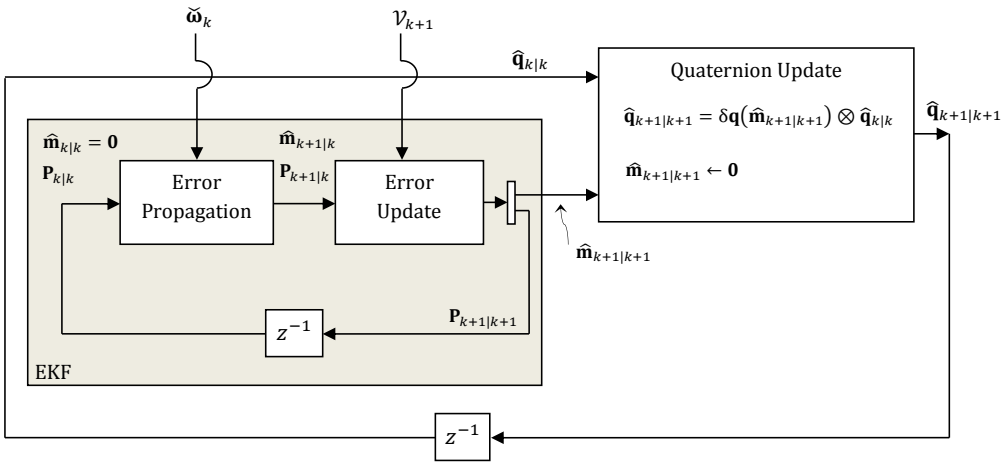

Fig. 4 Block diagram of the MEKF [15].

$$\mathbf{r} = \frac{\mathbf{p}^{(i)} - \mathbf{p}}{\|\mathbf{p}^{(i)} - \mathbf{p}\|}. \tag{7}$$

In order to compute $\mathbf{b}$ from the landmark image, consider the pinhole camera model [11], with focal length f, as illustrated in Fig. 3. Define the image coordinate system $S_{\mathrm{I}} \triangleq \{X_{\mathrm{I}}, Y_{\mathrm{I}}, Z_{\mathrm{I}}\}$ with origin at the camera center (see Fig. 3). For simplicity, assume that the camera center coincides with CM. From the image data, one can measure the S_{I} vector $\mathbf{b}_{\mathrm{I}} = [x_{\mathrm{I}}\ y_{\mathrm{I}}\ f]'$, which points from C to the landmark image on the image plane.

Now, define the S_{B} vector $\mathbf{b}_{\mathrm{B}}$ corresponding to $\mathbf{b}_{\mathrm{I}}$. It can be computed by $\mathbf{b}_{\mathrm{B}} = \mathit{\Gamma}\mathbf{b}_{\mathrm{I}}$, where

$$\mathit{\Gamma} \triangleq \begin{bmatrix} 1 & 0 & 0 \\ 0 & -1 & 0 \\ 0 & 0 & -1 \end{bmatrix}, \tag{8}$$

which is obtained by inspection of the relationship between S_{I} and S_{B}, as depicted in Fig. 3.

Finally, the S_{B} representation of the unit vector pointing from CM towards the landmark is given by

$$\mathbf{b} = \frac{\mathbf{b}_{\mathrm{B}}}{\|\mathbf{b}_{\mathrm{B}}\|}. \tag{9}$$

3.3 Module 3: Attitude Estimation

The method proposed here is based on the Multiplicative Extended Kalman Filter (MEKF) first introduced in [15]. To explain the MEKF, consider the block diagram of Fig. 4 and the following definitions. Denote the quaternion estimate at instant k by $\hat{\mathbf{q}}_{k|k}$. Let the MRP $\mathbf{m}(t)$ represent the true attitude error with respect to

the quaternion estimate $\hat{\mathbf{q}}_{k|k}$. Denote the MV filtered estimate of $\mathbf{m}(t)$ at instant $k+1$ by $\hat{\mathbf{m}}_{k+1|k+1}$ and the corresponding covariance matrix by $\mathbf{P}_{k+1|k+1}$. The attitude error estimate $\hat{\mathbf{m}}_{k+1|k+1}$ is computed by the continuous-discrete formulation of the extended Kalman filter (EKF) [3], considering the state model (5) and the measurement model (2)-(3), for $i = i_1, i_2, ..., i_n$ (indices of the visible landmarks at instant k). Now, in order to compute the quaternion estimate at instant $k+1$, $\hat{\mathbf{q}}_{k+1|k+1}$, the error estimate $\hat{\mathbf{m}}_{k+1|k+1}$ is incorporated into the previous quaternion estimate $\hat{\mathbf{q}}_{k|k}$ by the following multiplicative update scheme:

$$\hat{\mathbf{q}}_{k+1|k+1} = \delta\mathbf{q}\left(\hat{\mathbf{m}}_{k+1|k+1}\right) \otimes \hat{\mathbf{q}}_{k|k}, \tag{10}$$

where $\otimes$ denotes the quaternion multiplication and $\delta\mathbf{q}\left(\hat{\mathbf{m}}_{k+1|k+1}\right)$ denotes the quaternion error corresponding to the MRP error $\hat{\mathbf{m}}_{k+1|k+1}$ [21]. Finally, it is worth mentioning that, as soon as $\hat{\mathbf{q}}_{k+1|k+1}$ is computed, it becomes the new reference for the attitude error $\mathbf{m}(t)$ and, in this case, $\hat{\mathbf{m}}_{k+1|k+1}$ is reset before starting the next iteration of the filter. Note that the MEKF maintains the unit norm of its estimates by means of the multiplicative quaternion update of equation (10), since the quaternion multiplication of two unit quaternions results in a third unit quaternion.

In the present paper, the error update of the MEKF is modified. While the original version adopts a batch update, considering all the n pairs of vector measurements belonging to $\mathcal{V}_{k+1}$ at once, the novel version processes them sequentially, one at a time, according the to following algorithm:

$$\mathbf{m}^{(0)} = \hat{\mathbf{m}}_{k+1|k}, \tag{11}$$

$$\mathbf{m}^{(j)} = \mathbf{m}^{(j-1)} + \mathbf{K}^{(i_j)}\left(\check{\mathbf{b}}_{k+1}^{(i_j)} - \hat{\mathbf{b}}_{k+1}^{(i_j)}\right),\ j = 1, 2, ..., n, \tag{12}$$

$$\hat{\mathbf{m}}_{k+1|k+1} = \mathbf{m}^{(n)}, \tag{13}$$

where $\mathbf{m}^{(j)}$, $j = 1, 2, ..., n$, are auxiliary variables for storing the intermediate updated estimates, $\check{\mathbf{b}}_{k+1}^{(i_j)}$ is the S_{B} measurement taken from the i_jth landmark, and $\hat{\mathbf{b}}_{k+1}^{(i_j)}$ is the predicted value of the S_{B} measurement taken from the i_jth landmark. The latter is computed on the basis of model (2)-(3), considering $\mathbf{m}_k = \mathbf{m}^{(j-1)}$.

The modified method will be called by Multiplicative Extended Kalman Filter with Sequential Update (MEKFSU). Note that the new version is a convenient implementation for the paper's problem, in which the number of visible landmarks varies with time. In the MEKF, this variation would require an update with changing dimension.

4 Simulation and Results

The present section evaluates the accuracy and convergence rate of the MEKFSU method using Monte Carlo simulations. The Simulink 3D Animation environment is adopted for simulating artificial camera images.

Table 1 Simulation scenarios.

Case	ϖ (rad/s)	a (rad/s)
1	10	$2\pi/180$
2	5	$2\pi/180$
3	2	$2\pi/180$
4	10	$6\pi/180$
5	5	$6\pi/180$
6	2	$6\pi/180$
7	10	$12\pi/180$
8	5	$12\pi/180$
9	2	$12\pi/180$

4.1 Simulation of the True Movement and Environment

For simplicity, the vehicle's movement is simulated in the Simulink environment only in its attitude kinematics, modeled by equation (5), considering that it is excited by a sinusoidal angular velocity of the form:

$$\boldsymbol{\omega}_k = \begin{bmatrix} a\sin(\varpi T_s k) \\ a\cos(\varpi T_s k) \\ a\cos(\varpi T_s k) \end{bmatrix}, \tag{14}$$

where ϖ is the frequency, a is the amplitude, T_s is the sampling time. It is worth emphasizing that for computing the vector measurements, the vehicle's position have to be known (see equation (7)). In a practical situation, this information could be provided by a GPS receiver, for example. Here, without loss of generality, the position is considered constant just to simplify the simulation of the artificial images.

In the Simulink 3D Animation environment, we implemented a graphical visualization of a quadrotor with its attitude varying according to (5) with velocities given by (14). Fig. 5(a) depicts it. Color landmarks were placed on the floor of this virtual environment. Table 2 lists the colors and respective positions chosen for the landmarks. A total of nine landmarks are taken into consideration in our simulations. For simulating the sequence of images, a virtual camera is placed at the vehicle's position. Fig. 5(b) shows one image read from the Simulink 3D Animation when S_{B} is exactly aligned with S_{R}. For simplicity and easy visualization, the virtual quadrotor is fixed at the position $\mathbf{p} = [0 \;\; 0 \;\; 1]'$ m. The sequence of artificial images is processed in the Simulink environment for detecting and identifying the visible landmarks at each sample time (note that since, in our illustration of the proposed method, the artificial images are noise-free and the landmarks have exactly known colors and positions, the detection and identification processing are straightforward). A sampling rate of 30 frames per second (FPS) is considered.

For evaluation, nine different combinations of ϖ and a are taken into account, as reported in Table 1. The covariance matrices of the noise terms on the angular velocity measurements and on the vector measurements are set with the values $\mathbf{Q} = (0.0005)^2\mathbf{I}_3$ (rad/s)^2, $\mathbf{R}_{b,k}^{(i)} = (0.001)^2\mathbf{I}_3$, and $\mathbf{R}_{r,k}^{(i)} = \mathbf{0}_{3\times 3}$.

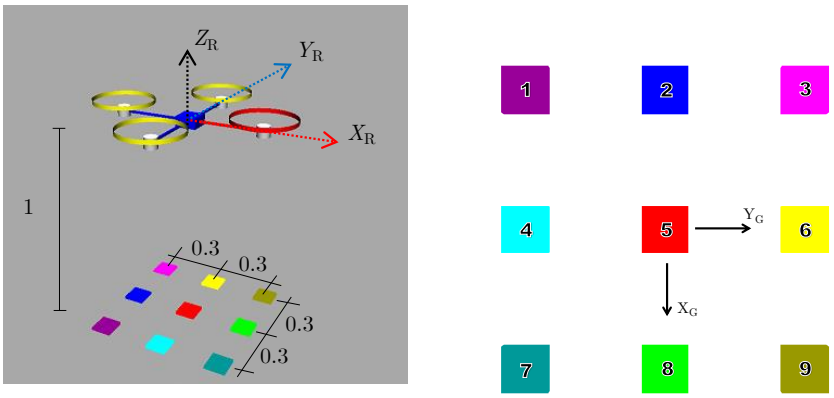

(a) (b)

Fig. 5 (a) The simulation environment using Simulink 3D Animation and (b) the camera point of view.

Table 2 The color and position of the landmarks.

Landmark	Color (R;G;B)	S_G Position (x;y;z)
1	(153;0;153)	(-0.3;-0.3;0)
2	(0;0;255)	(-0.3;0;0)
3	(255;0;255)	(-0.3;0.3;0)
4	(0;255;255)	(0;-0.3;0)
5	(255;0;0)	(0;0;0)
6	(255;255;0)	(0;0.3;0)
7	(0;153;153)	(0.3;-0.3;0)
8	(0;255;0)	(0.3;0;0)
9	(153;153;0)	(0.3;0.3;0)

Table 3 Monte Carlo simulation parameters.

Initial true attitude in MRP	$\mathbf{m}_0 = \begin{bmatrix} 0 & 0 & 0 \end{bmatrix}'$
Covariance of the initial attitude error	$\mathbf{P}_0 = (12)^2\mathbf{I}_3$
Initial estimated attitude in MRP	$\hat{\mathbf{m}}_{0\|0} \sim \mathcal{N}(\mathbf{m}_0, \mathbf{P}_0)$ [1]
Sampling period	$T_s = 0.001$ Hz
Number of Monte Carlo runs	MC = 100
Simulation time	$T = 10s$

4.2 Evaluation

The MEKFSU method is evaluated on the basis of a Monte Carlo (MC) simulation for each of the nine cases shown in Table 1. The adopted MC simulation parameters are given in Table 3.

[1] This notation means that $\hat{\mathbf{m}}_{0|0}$ is a realization of a Gaussinan random vector with mean and covariance of $\mathbf{m}_0$ and $\mathbf{P}_0$, respectively.

Table 4 Attitude estimation results.

Case	ϖ (rad/s)	a (rad/s)	max $\bar{\epsilon}_k$ (degree)
1	10	$2\pi/180$	0.5694
2	5	$2\pi/180$	0.6229
3	2	$2\pi/180$	0.7366
4	10	$6\pi/180$	0.9059
5	5	$6\pi/180$	1.2640
6	2	$6\pi/180$	2.0000
7	10	$12\pi/180$	1.6470
8	5	$12\pi/180$	2.3730
9	2	$12\pi/180$	4.1570

In order to measure the accuracy of the filter, the following figure of merit is considered:

$$\epsilon_k = \text{acos}\left(\frac{1}{2}\text{tr}\left[\mathbf{D}(\mathbf{q}_k)\mathbf{D}(\hat{\mathbf{q}}_{k|k})'\right] - \frac{1}{2}\right), \tag{15}$$

where $\mathbf{D}(\mathbf{q}_k)$ is the true attitude matrix and $\mathbf{D}(\hat{\mathbf{q}}_{k|k})$ is the corresponding attitude matrix estimate. Note that $\epsilon_k \geq 0$ consists of the principal Euler angle corresponding to the error attitude matrix given by the product $\mathbf{D}(\mathbf{q}_k)\mathbf{D}(\hat{\mathbf{q}}_{k|k})'$.

Figures 6–8 show the MC averages $\bar{\epsilon}_k$ and standard deviations $\sigma_{\epsilon,k}$ of ϵ_k for the nine simulation cases established in Table 1. Moreover, Table 4 shows the maximum values for $\bar{\epsilon}_k$. One can see that by decreasing the frequency ϖ of variation of the angular velocity, the filter accuracy is reduced. This is explained by the loss of observability due to the slow variation of the vector measurements with time when the vehicle is moving slowly. On the other hand, one can also observe a loss of accuracy as the amplitude a of variation of the angular velocity is increased. This is because the number of visible landmarks descreases as the amplitude a is increased; a smaller number of landmarks implies in a smaller amount of data and, consequently, in a reduced observability. Based on Table 4, one can see that, for small amplitudes a (and, consequently, for a large amount of visible pairs of vector measurements), in average, it is possible to obtain an accuracy better than one degree, which is sufficient for multirotor aerial vehicles.

Although we have not evaluated the proposed method for different values of camera FPS, in general, the performance of any stochastic estimator, recursive or not, is always improved by increasing this parameter, since it implies in a larger amount of measurement data in a certain period of time. This can be justified by the well-known Law of Large Numbers [18]. In other words, with a faster camera, one would expect a better performance of the MEKFSU.

5 Conclusion and Future Work

The present paper has proposed a new method for determining attitude from vector measurements taken from a single downward-pointing camera attached on a vehicle that navigates in an environment with known landmarks. The method can be viewed as an effective complement to the conventional ones which are based on magnetometers and inertial sensors. The idea of the method was taken from the

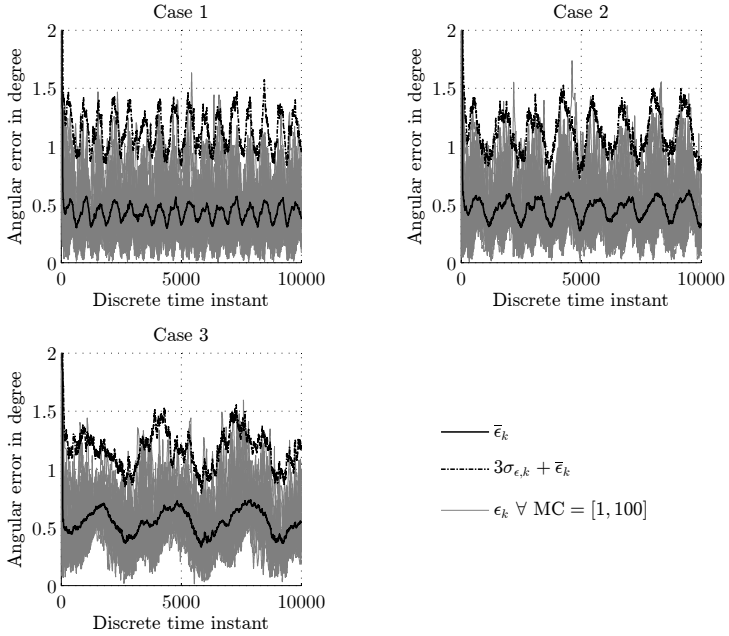

Fig. 6 Attitude error for cases 1–3.

aerospace literature, where attitude determination from vector measurements for space vehicles is a mature topic. In space, the vector measurements are taken with a variety of sensors (solar sensor, magnetometer, star sensor, horizon sensor, etc.). For aerial robot applications, typical sensors available for attitude determination are the magnetometers (to measure the local magnetic field) and accelerometers (to measure the gravitational acceleration). In general, such methods suffer from two disadvantages. First, the accelerometers only measure the difference between the total acceleration and gravity. Then, in order to measure the gravitational acceleration (as a vector measurement), one needs to assume that the vehicle does not accelerates, which may not always be true, e.g., in curves. Second, in environments where an aerial robot typically operates (low altitude and indoors), the local magnetic field can suddenly change in such a way that one cannot predict its value in the reference coordinate system. This work shows that with a single camera, one can take as many vector measurements as the number of visible landmarks. The proposed method was structured in three modules: 1) landmark detection and identification; 2) vector measurement computation; and 3) attitude estimation. The main contributions of the paper are the modular framework itself and a new attitude estimation method, named multiplicative extended Kalman filter with sequential update (MEKFSU). The MEKFSU differs from the well-known MEKF in that, at each sampling time, the former processes the available pairs of vector measurements in a sequential form, one pair at a time. We argue that this is a convenient implementation, since the number of visible landmarks (and then, the number of available pairs of vector measurements) can vary with time.

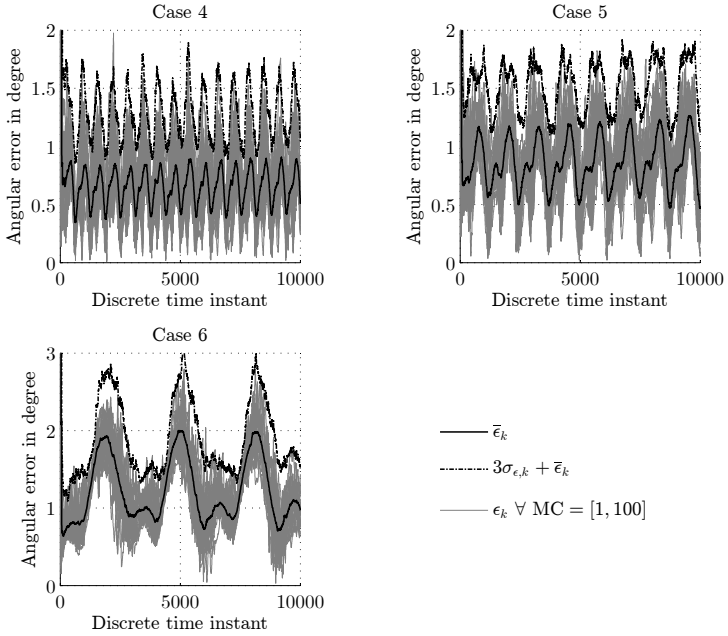

Fig. 7 Attitude error for cases 4–6.

In this case, the MEKF would require an implementation in which the filter update changes its dimension along the time. Monte Carlo simulations showed that the proposed method is effective and provides estimates sufficiently accurate for multirotor aerial vehicles.

References

1. Bar-Itzhack, I.Y.: Request - a recursive quest algorithm for sequential attitude determination. Journal of Guidance, Control and Dynamics **19**, 1034–1038 (1996)
2. Bar-Itzhack, I.Y., Oshman, Y.: Attitude determination from vector observations: Quaternion estimation. IEEE Transactions on Aerospace and Electronic Systems **21**, 128–136 (1985)
3. Bar-Shalom, Y., Li, X.R., Kirubarajan, T.: Estimation with Applications to Tracking and Navigation. John Wiley & Sons, New Jersey (2001)
4. Carrillo, L.R.G., Lopez, A.E.D., Lozano, R., Pegard, C.: Combining stereo vision and inertial navigation system for a quad-rotor uav. Journal of Intelligent and Robotic Systems **65**, 373–387 (2012)
5. Cheviron, T., Hamel, T., Mahony, R., Baldwin, G.: Robust nonlinear fusion of inertial and visual data for position, velocity and attitude estimation of uav. In: IEEE International Conference on Robotics and Automation. Roma, Italy (2007)
6. Choukroun, D., Bar-Itzhack, I.Y., Oshman, Y.: Optimal-request algorithm for attitude determination. Journal of Guidance, Control and Dynamics **27**, 418–425 (2004)
7. Erginer, B., Altug, E.: Modeling and pd control of a quadrotor vtol vehicle. In: IEEE Intelligent Vehicles Symposium. Istanbul, Turkey (2007)
8. Farrell, J.L.: Attitude determination by kalman filtering. Automatica **6**, 419–430 (1970)
9. Gebre-Egziabher, D., Elkaim, G.H.: MAV attitude determination by vector matching. IEEE Transactions on Aerospace and Electronic Systems **44**, 1012–1028 (2008)

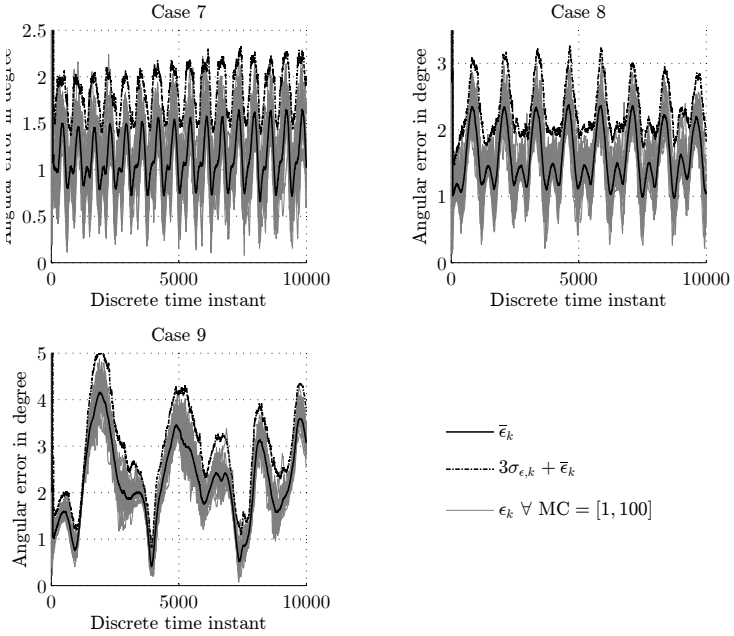

Fig. 8 Attitude error for cases 7–9.

10. Gonzalez, R.C., Woods, R.E.: Digital Image Processing. Pearson Education (2009)
11. Hartley, R., Zisserman, A.: Multiple View Geometry in Computer Vision. Cambridge University Press, New York (2004)
12. Hoffmann, F., Goddemeier, N., Bertram, T.: Attitude estimation and control of a quadrocopter. In: IEEE/RSJ International Conference on Intelligent Robots and Systems. Taipei, Taiwan (2010)
13. Huang, Y., Thomson, S.J., Hoffmann, W.C., Lan, Y., Fritz, B.K.: Development and prospect of unmanned aerial vehicle technologies for agricultural production management. International Journal of Agricultural and Biological Engineering pp. 1–10 (2013)
14. Kim, C., Kim, T., Lyou, J.: Realization of a mems attitude reference system for a small aerial vehicle. In: IEEE Annual Conference on Industrial Electronics (IECON). Montreal (2012)
15. Lefferts, E.J., Markley, F.L., Shuster, M.D.: Kalman filtering for spacecraft attitude estimation. Journal of Guidance, Control and Dynamics **5**, 417–429 (1982)
16. Mancini, F., Dubbini, M., Gattelli, M., Stecchi, F., Fabbri, S., Gabbianelli, G.: Using unmanned aerial vehicles (uav) for high-resolution reconstruction of topography: The structure from motion approach on coastal environments. Remote Sensing pp. 6880–6898 (2013)
17. Oltmanns, S.O., Marzolff, I., Peter, K.D., Ries, J.B.: Unmanned aerial vehicle (uav) for monitoring soil erosion in morocco. Remote Sensing pp. 3390–3416 (2012)
18. Papoulis, A., Pillai, U.: Probability, Random Variables and Stochastic Processes. McGraw-Hill (2002)
19. Santos, D.A., Saotome, O., Cela, A.: Trajectory control of multirotor helicopters with thrust vector constraints. MED (2013)
20. Shabayek, A.E.R., Demonceaux, C., Morel, O., Fofi, D.: Vision based uav attitude estimation: Progress and insights. Journal of Intelligent and Robotic Systems **65**, 295–308 (2012)
21. Shuster, M.D.: A survey of attitude representations. Journal of the Astronautical Sciences **41**, 439–517 (1993)
22. Shuster, M.D., Oh, S.D.: Three-axis attitude determination from vector observations. Journal of Guidance, Control and Dynamics **4**, 70–77 (1981)

23. Tarhan, M., Altug, E.: Ekf based attitude estimation and stabilization of a quadrotor uav using vanishing points in catadioptric images. Journal of Intelligent and Robotic Systems **62**, 587–607 (2011)
24. Tayyab, M., Farooq, U., Ali, Z., Imran, M., Shahzad, F.: Design of a blimp based unmanned aerial vehicle for surveillance. International Journal of Engineering and Technology (IJET) pp. 519–530 (2013)
25. Wahba, G.: A least-squares estimate of satellite attitude. SIAM Reviews **7**, 409 (1965)
26. Wang, S., Yang, Y.: Quadrotor aircraft attitude estimation and control based on kalman filter. In: 31st Chinese Control Conference (CCC). Hefei, China (2012)
27. Wertz, J.R.: Spacecraft Attitude Determination and control. Kluwer Academic Publishers, The Netherlands (1978)